NGU Rapport 97.176

The Agip NSD-1 well at Tananger

NGU
Norges geologiske undersøkelse
Geological Survey of Norway

Postboks 3006 - Lade
7002 TRONDHEIM
Tlf. 73 90 40 11
Telefaks 73 92 16 20

RAPPORT

Rapport nr.: 97.176	ISSN 0800-3416	Gradering: Åpen

Tittel: The Agip NSD-1 well at Tananger	
Forfatter: Tore Herrevold	Oppdragsgiver: NGU, Norsk Agip A/S
Fylke: Rogaland	Kommune: Sola, Stavanger og Sandnes
Kartblad (M=1:250.000)	Kartbladnr. og -navn (M=1:50.000) Stavanger 1212 IV
Forekomstens navn og koordinater:	Sidetall: 32 Pris: kr. 75,- Kartbilag: 2

Feltarbeid utført: Mai -95	Rapportdato: 28. november 1997	Prosjektnr.: 61.2337.00	Ansvarlig: Øystein Nordgulen

Sammendrag:

Geological description of well logs, cuttings and surface samples in the Tananger-Sandnes area was carried out in order to gain a wider understanding of the Caledonian nappe sequences.The upper part of the Jæren Nappe Complex comprises gneisses, amphibolite, marble and calc-silicate gneiss. This may be equivalent to the mica gneiss and minor calcite marbles seen in the NSD-1 well. A log break at around 550 m may correlate with the contact between the upper and middle parts of the nappe complex. The fault zone separating the middle and lower parts is most probably located in the interval 900-950 m, but is difficult to detect in log interpretations. Below this level the dominant rock-types are more granitic compared with those above. The NSD-1 well does not penetrate the contact between the Jæren Nappe Complex and the basement.

Emneord: Geologisk undersøkelse	Elektriske logger	Borhullsloggingl
Borkaks		

INNHOLD

FIGURER

TABELLER

VEDLEGG

APPENDIX 1
APPENDIX 2

1. INTRODUCTION

The NSD-1 borehole is situated at Tananger west of Stavanger, and was drilled in 1989-90 by Norsk Agip A/S in connection with a planned training facility for drilling engineers. It was drilled to a measured depth of 1241m below the surface and has an inclination towards NE. Upon completion of the drilling the well was put at the disposal of the two logging companies Western Atlas and Schlumberger for some days for the demonstration of logging technology. All of the material obtained during these operations was handed over to the Geological Survey of Norway in order to include lithological and structural information from the drillcore in a general understanding of the bedrock geology of the Jæren area. The well transects rocks belonging to the Caledonian Jæren Nappe Complex.

Well logs include; dual caliper, gamma ray and NGS-ratios, neutron porosity, bulk density, array sonic, formation micro scanner (FMS), and borehole televiewer log data.

The data from the borehole have previously been interpreted by Knut Kirkemo at Norsk Agip A/S assisted by multivariate statistical analysis performed by Kazimir Mansnich of Shclumberger (Fig. 1). Harald Brekke and Fridtjof Riis, both of NPD, contributed significantly with discussions of the local geology. The log curves and cuttings were interpreted as mica gneisses down to ca 550 m, alternating granodiorites and granites (called granulites) from 550 m to 900 m, and from 900 m and down to the bottom of the borehole the rocks were interpreted to be granodiorites and granites, including a thin layer of marble at about 1080 m.

1.1 General geology

The allochthonous rocks of the Jæren area comprise three tectonic units that rest upon the Precambrian basement (Fig. 2). The lowermost nappe is dominated by phyllites with layers of metaclastic rocks (Birkeland 1981). These rocks are complexly folded and in the central area of the Stavanger peninsula there is large-scale folding along NW-SE trending axes. The fold structures are strongly compressed and have steep to vertical axial planes. The next, overlying unit consists of heterogeneous gneisses and feldspathic schists. The contact between these units has been a locus of shearing, probably a result of the recumbent folding that has affected rocks of both units. These two nappes are overlain by the Jæren Nappe Complex which is composed of medium amphibolite-facies supracrustal rocks and granitoids, of anatectic derivation. Deformation in this unit is reflected in a N-S trending sinuous fold system with the foliation deflected around granitoid plutonic rocks that mark the termination of the nappe sheet towards the northeast. Rocks of lower greenschist-facies metabasites that are found on small islands further west and northwest of Jæren are thought to represent the highest

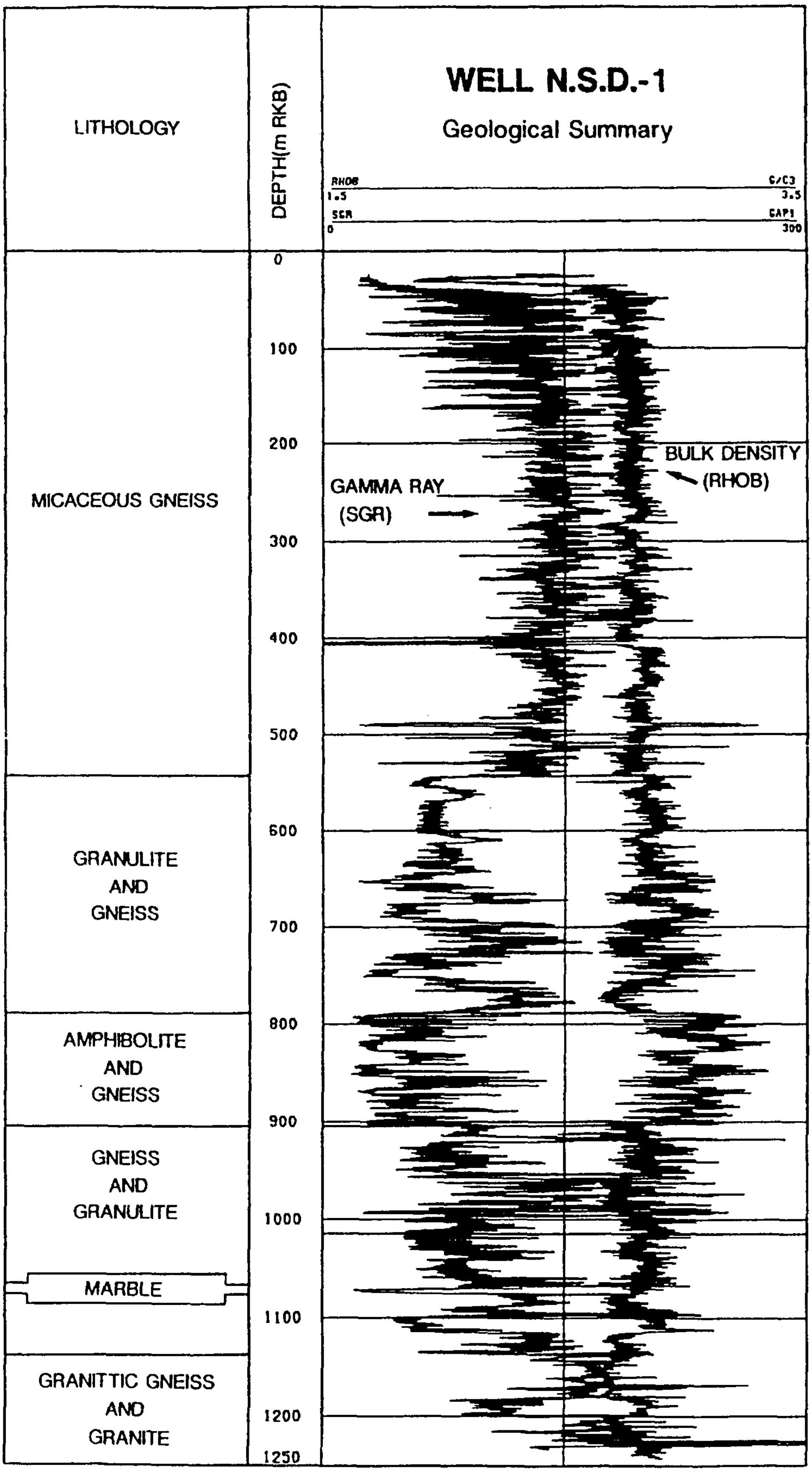

Fig. 1. *Geological summary of the Agip NSD-1 well at Tananger. This interpretation by Knut Kirkemo (Norsk Agip), has been published in the description presented on the 1:250,000 map-sheet Stavanger (Jorde et al. 1995).*

tectonic unit within the nappe system (Birkeland 1975). These rocks display of fold axes trending N-S and NNE-SSW, i.e. approximately parallel to the front of the Caledonian orogen in this region.

1.2 Procedure

In order to gain a better geological understanding of the area, which would also help in interpreting the well log data, fieldwork and sampling were carried out in the area around the well. Thin-sections were prepared both from these samples and from the cuttings at different intervals in the borehole based on rapid binocular studies. After mineralogical determination of the different rock types found in thin-sections of the cuttings, the data were correlated with the electrical well logs, and new interpretations of the log curves were carried out.

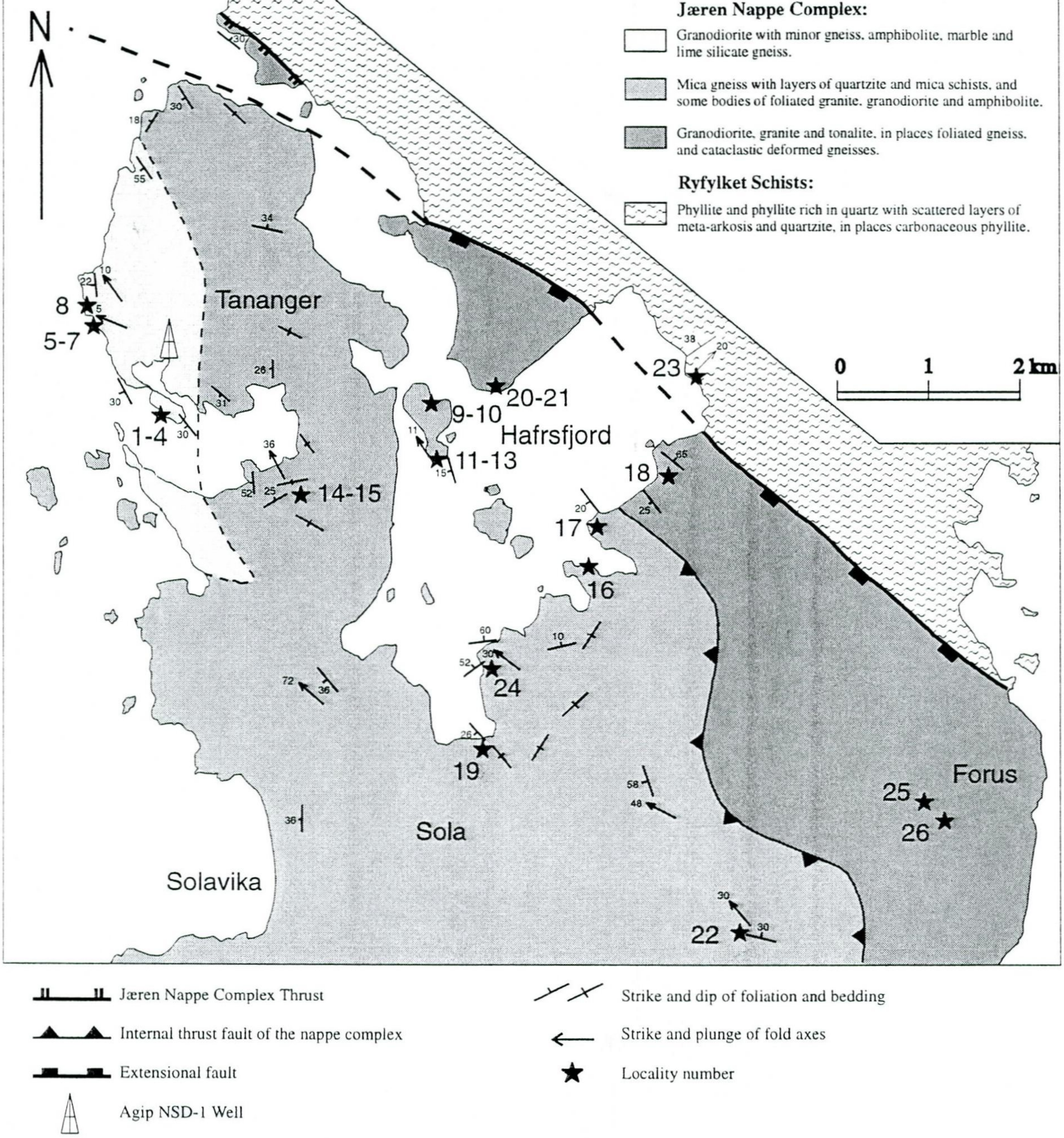

Fig. 2. Simplified geological map of the Tananger area (based on Jorde et al. 1995). Sample localities are numbered.

2. SURFACE SAMPLES

Surface samples were collected from the different lithologies present in the area. These include:

- Tananger leucogranite; with inclusions of gneiss, amphibolite and marble.
- Jæren formation; comprising quartz-feldspar gneisses, banded gneisses, (garnet)-amphibole schists, (garnet)-mica schists, amphibolites and marbles.
- Madla formation; magmatic rocks of tonalitic and enderbitic composition.

The Tananger leucogranite, appearing as a more or less dense network of sills and dykes of pegmatite and leucogranite, has intruded the country rock which consists of quartz-feldspar gneisses, biotite schists, amphibolites, calcite marbles and calc-silicate gneisses. The marbles are intercalated with different types of gneiss, amphibolite and meta-arkose. Fig. 2 shows the general geology in the area and the localities where rock samples have been taken. Thin-section data are summarised in Table 1, while a short description of the samples is given in Appendix 1.

3. CUTTINGS

Drilling data

Mixing of rock cuttings during their transportation to the surface makes the use of cuttings as boundary indicators inappropriate. The rate of penetration measured through the drilling process was low and quite uniform (approx. 0.75-1.5 m/hr) and does not serve to identify rock boundaries.

4. WELL LOGS

4.1 Logging tool response

The radiation recorded in the gamma ray log emanates from naturally occurring uranium, thorium and potassium (Table 2). Most rocks are radioactive to some degree, and igneous and metamorphic rocks more so than sediments (Table 3).

Both uranium and thorium originate in the acid-to-intermediate igneous rocks, but their distribution is very irregular since they are associated with accessory minerals such as apatite.

Sample	Quartz	K-feldspar	Plagioclase	Green hornblende	Pyroxene	Garnet	Biotite	Epidote	Muscovite	Zoisite/clinozoisite	Calcite	Titanite	Apatite	Opaques	Rock type
1	35	35	25				a	1	1						porphyritic granite
2			25	70			1-2	a				a			amphibolite
3	40	15-20	20-25	1-2				a				a			leuco granodiorite
4	10	10	<1	1			<1	75			1-2				calcsilicate rock
5	50	10	30				2		a	5		a			granodioritic, aplitic vein
6	60-65	1	a				10			15-20	a	a	a	a	feldspathic quartz mica gneiss
7			30-40	50			2-4					a	a	2-3	amphibolite
8	45	30	1-2	10			a	10			a		a	a	alkali feldspar granite
9	70-80			3-5		<5		15-20						<1	meta-arkose
10	1-2		a	85-90		5-10								1	garnet amphibolite
11	a	a	a					a		a	>95		a		limestone marble
12	35-40	5	25-30	12-15		<1	<1				5-8	a	<1	a	tonalite - trondhjemite
13			40					55		5					meta-volcanite ??
14	55-60	a	5				8-10		5-6				a	a	muscovite biotite gneiss
15	50	5	40			a			2-3				a	a	aplitic vein
16	10-15			80-85			a					a		2-3	amphibolite schist
17	50-55	3-4	2-3	15-20		5-6	15					1	1		garnet-hornblende amphibolite
18	25-30	40-45	10				5		8-10		a		a		granodiorite
19	30		5-10				a		a	a	60			a	lime silicate gneiss
20			75-80		a		a			a				20-25	porphyritic diabase
21	30	8-10	50				5-7			3			a	a	tonalitic gneiss ??
22	40	10	25				10-15	10					a		granodiorite
23	70								25					5	phyllite
24	30		40				10	a	15	a			a	a	meta-tonalite
25	40	20	35				a		a		a			<1	monzo-granitic gneiss
26	25		55				3-4			a			a	a	tonalitic gneiss

Table 1. Thin-section data from surface samples in the Tananger area. Mineral content is given in volume (a - accessory). The sample numbers refer to map localities in Fig. 2.

Potassium is present, especially in the acid igneous rocks, principally in the alkali (potassic) feldspars. The net result is that basic igneous rocks have low radioactivity, while the intermediate and acid types show progressively higher values (Keys, 1979, Sanyal et al. 1980) (Table 2).

The logging tool response values for gamma ray, density tool and neutron porosity are shown in Table 3.

Rock type	Th (ppm)	U (ppm)	K_2O %	Typical radioactivity
Acid intrusive	1-25	1-8	4.11-2.00	High
Acid extrusive	9-25	2-7	2.00-6.00	High
Basic intrusive	0.5-	0.3-2	0.90-2.20	Low
Basic extrusive	0.5-10	0.2-4	1.40-2.50	Low
Ultrabasic	-	0.0001-0.03	1,60	Very low

Table 2. Radioactive elements in igneous and volcanic rocks (from Serra et al. 1980).

Rock types and minerals	Gamma Ray, API	Density tool, g/cm^3	Neutron Porosity Units
Basalt	12-24	2.7-3.2	
Granite	24-96	2.52-2.8	
Gneiss	24-48	2.6-3.04	
Quartz		2.64-2.66	-2,00
Calcite		2,71	-1,00
Glauconite	75-90	2.2-2.8	38,00
Muscovite	140-270	2.76-3.1	20,00
Biotite	90-275	2.65-3.1	21,00
Microcline	220-280	2.52-2.57	-3,00
Orthoclase	220-280	2.53-2.63	-3,00

Table 3. Logging tool response values. All values are shown so that they cover the range of values found in the various sources, i.e. none of the sources has values outside those listed above. Data from Rider (1986) based on Serra (1972, 1979), Dresser Atlas (1983), Gearhart (1983) and Schlumberger (1985).

4.2 General description of the NSD-1 logs

Figs. 3 and 4 show the different gamma logs, bulk density and neutron porosity logs available for the interval 475-1230 m. The interval above 475 m has been omitted on the figure, partly due to its homogeneous character and also to save space. The complete succession is seen in the compressed logs in Fig. 1 where the section above 475 m has been interpreted to represent fairly homogeneous micaceous gneiss.

Considering the electrical logs, it is most convenient to divide them into two sections; above 545 m and below 545 m, here called *Log section I* and *Log section II*, respectively. The reason for this is that there is a clear difference in log response above and below this level of depth, and this is especially evident on the gamma ray log (SGR) and the thorium and potassium log, as explained below.

Log section I (above 545 m)
In the interval from 45 m down to 54 m the gamma ray readings are generally high, but with numerous alternations in between 115 and 150 API. The readings are especially consistent from about 140 m and downwards. From the surface and down to 140 m the gamma ray values alternate more strongly between higher and lower readings (50-75 API) (Fig. 1).

The thorium content seems to vary between 16 and 20 ppm down to 545 m. Below this depth it abruptly drops to 6-10 ppm and remains consistent through the next approximately 100 m (Fig. 3). In the upper part of *Log section I* the thorium readings alternate more rapidly in the same manner as the gamma readings down to about 140 m.

A major drop in the gamma readings is seen over the minor interval 488-492 m, where values are of 30 API. This drop is reflected in the thorium and potassium logs with values less than 4 ppm for thorium and with potassium values of 0.0025 unit %. The bulk density log, in contrast, makes a very high peak reading of 3.30 % compared to a mean value around 2.75 %. The caliper log does not have any marked caving at this particular point, which could explain the anomalous values.

The bulk density log also has some very low readings at 145 m, 255 m, 379 m and at 404-407 m. These are not reflected in the other logs, except for the low at 404-407 m. This last interval is also marked by a larger cavity seen on the caliper log. This cavity represents a very sharp and confined break and may represent a cave-out due to very weak lithology, possibly a fault zone.

On the uranium log two distinct peaks are seen, one at 378-382 m and another at 513 m. Both peaks indicate a uranium content about 17 ppm which is very high compared with the average of 3-4 ppm.

Log section II (below 545 m)

From 545 m and down to 675 m the gamma log (SGR) is generally low with values in the range of 60-90 API, although there is an increase over the last 40 m (Fig. 3). In this interval of 130 m both the thorium and the potassium readings are generally low, but with an increase towards the base. The uranium content is generally very low, being around 2 ppm.

The interval 675-790 m is characterised mainly by two larger, highly serrated peaks in the gamma log. These reflect high readings in thorium and potassium contents. The uranium log is generally low, but shows a weak increase over these peaks. In between, from 675 to 695 m, the gamma readings are low and accompanied by very high bulk density readings. This is also the case for the interval 730-750 m although the gamma readings are not so consistent here. From 745 m to 750 m the neutron porosity is extremely high with a peak at ca 0.25 NPU. A narrow cavity marked by the caliper log may partly explain this high porosity value.

From 790 to 903 m the gamma log is fairly irregular with low base level and an abundance of narrow peaks. This interval is also characterised by very high bulk density values. Thorium and potassium logs are quite serrated but generally with low values. The uranium content is hardly detectable and only small peaks are shown, while the neutron porosities are generally high in the range of 0.0 to 0.15 NPU. The caliper shows very little caving in this interval.

From 903 m and down to the end of the log at 1130 m the column is characterised by moderate to high gamma readings and with only minor intervals with very high and very low readings. The narrow interval from 915 to 921 m is marked by an extremely high gamma peak (275 API), reflecting a very high thorium content (50 ppm) and a minor uranium peak (5 ppm).

The interval 921 to 950 m exhibits moderate gamma values, interrupted only by a narrow break at 992-994 m where the log shows very low readings.

From 950 m to 997 m the gamma log is very serrated but with generally very high peaks. Below this, down to 1098 m, the thorium and potassium logs show moderate levels, but with slightly higher levels in the intervals 1000-1012 m, 1035-1042 m, 1060-1072 m and 1075-1100 m. In addition, there are some extreme readings of thorium and uranium contents at 1015 m and 1096-1097 m. Two breaks with low values are found at 992-994 m and at 1073-1075 m. At 992-994 m the break is accompanied by higher readings in neutron porosity and very high readings of bulk density. The break at 1073-1075 m is not marked by any change in porosity and density values.

Low values in the thorium and potassium logs are found in the interval 1098-1114 m where the gamma readings are consistently low (Figs. 3 and 4). The uranium content is very low over this interval. From 1114 m to 1133 m the gamma readings are generally high, with slightly higher values from 1136 down to 1182 m. At the beginning of this last interval the uranium content is quite high but decreases downwards. In between there is a narrow low interval at 1133-1136 m. The uranium log has some peaks at 1168 m, 1170 m and 1180 m which correspond with high peaks in the gamma log. From 1183 to 1198 m there is another interval of high gamma readings followed by an interval from 1198 to 1230 m with slightly higher values, similar to that at 1136-1182 m. The uranium readings are low to moderate, but tend to increase downwards. Some peaks are found at 1205 m, 1210 m and from 1225 to 1230 m.

Formation Micro Scanner Log

This type of log is only available from the intervals 899 - 908 m and 1200-1222 m. Fractured intervals are clearly visible, and the most pronounced are the intervals 899-903 m, 905-908 m, 1200-1202 m and 1213-1218 m. No offsets are detectable.

Borehole Televiewer Log

Data from this log are available in the interval 1041-1129 m, and fractured intervals (nf = number of fractures in the interval) have been counted:

1041 m, nf = 2
1048-1049 m, nf = 2
1050-1055 m, nf = 6-7
1057-1058 m, nf = 1
1060 m, nf = 2
1065 m, nf = 2, very high gamma readings
1070-1075 m, nf = 6, break in log at 1072 m; gamma high above and low below
1106-1114 m, change in bedding; interval with higher dips
1123-1129 m, nf = 3-4, weakly disturbed

5. INTERPRETATION OF WELL LOGS AND CUTTINGS

The electrical well logs were divided into different intervals based on log tool response values and characteristics. These were then correlated with thin-section data from the same intervals. The cutting samples give an overall picture of the different rock types that occur over an interval of the borehole of several metres. The sampled interval was taken to represent a certain rock type if this was the dominating constituent of the sample. Interpretation of cuttings from the rock types present in the well is problematic due to the fact that the cuttings are smaller than the mineral aggregates of the bedrock. Further, the rocks are finely layered and the mineralogy of the layers varies considerably.

A generalised interpretation of the lithology based on cuttings and well logs is presented on the left side of the logs in Figs. 3 and 4. Based on these interpretations the corresponding log response values are shown in Table 4.

Some layers of calcitic marble in the uppermost part of the succession (Fig. 5) have been recognised based on log response values from the thin zone of calcite marble at 1075 m. These zones are quite similar to the amphibolitic horizons in terms of gamma ray response, e.g. low in the area 20-70 API. A slight difference, however, is seen in the neutron porosity and bulk density logs, where amphibolites tend to show somewhat higher values than the calcite marbles.

Extremely high peaks of uranium occur at several levels which may infer possible the presence of fault zones. This is difficult to verify, however, due to lack of cavings and anomalous density and porosity values.

The formation micro scanner (FMS) log indicates fractures at around 900 m. This coincides with the change from tonalitic gneiss to an overlying highly heterogeneous sequence of alternating amphibolites and tonalitic gneisses. This discontinuity probably reflects a fault zone, but the nature of the zone is unknown. A similar case is seen in the FMS log at around 1200 m where fracturing coincides with

LITHOLOGY	Gamma (SGR) API	U ppm	K % unit	Th ppm	Neutron Porosity (NPHI)	Bulk Density g/cm3
Granite	120-180	0-4	0.035-0.05	10-20	0-3	2.65-2.8
Granitic gneiss, porphyric	135-175	0,00	0.04-0.06	20-28	0,00	2.7-2.8
Granitic biotite gneiss	150-225	3-8	0.03-0.05	12-20		
Tonalitic gneiss	60-105	0-4	0.015-0.035	5-12	1.5-4.5	2.8-2.9
Tonalitic gneiss rich in hornblende	45-75	0-2	0.02-0.03	3-6		
Mica gneiss	120-180	1-6	0.02-0.045	16-22	0,70	2.75-2.85
Garnet bearing quartz rich mica gneiss	90-135	1-3	0.025-0.035	8-14		
Amphibolite	25-70	0-2	0.005-0.025	2-4	3-12	3-3.4
Calcite marbles	20-60	0-1.5	0.01-0.015	0-4	0-1.5	2.65-2-80

Table 4. The interpreted rock types based on cutting analyses from the Agip NSD-1 well, and their corresponding logging tool response values.

the change from underlying granite biotite gneiss to overlying garnet-bearing quartz-rich mica gneiss. The borehole televiewer log shows fracturing in the interval 1070-1075 m that coincides with a thin horizon of calcite marble. This is most probably due to a difference in competence between the surrounding granite and the marble.

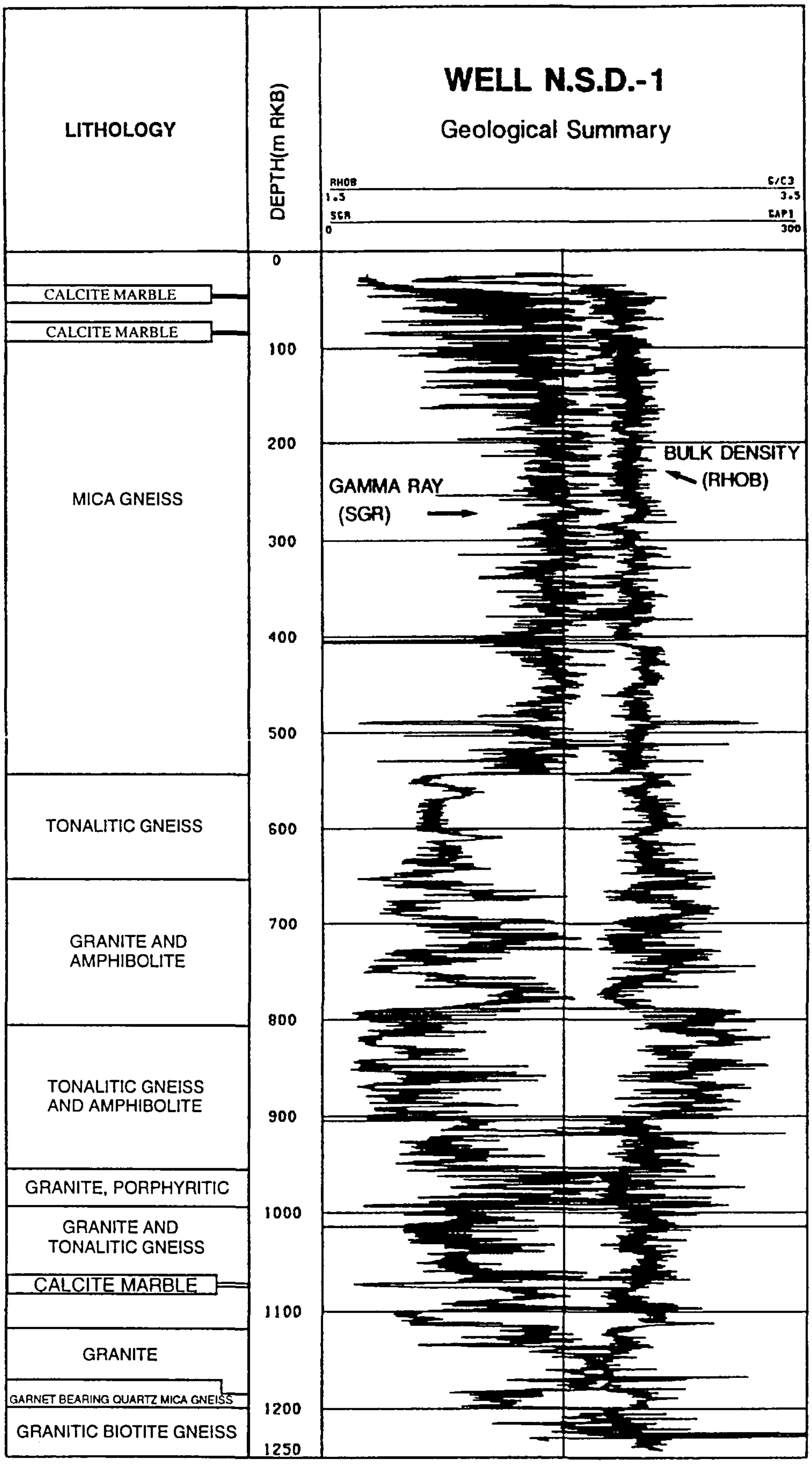

Fig. 5. Reinterpretation of the well log data represented as a geological summary.

6. CONCLUSIONS AND DISCUSSION CONCERNING WELL LOG INTERPRETATION AND CORRELATION OF THE SURFACE GEOLOGY

Detailed interpretation of the well logs and cutting analyses are given in Figs. 3 and 4, while a geological summary is given in Fig. 5, which is a revised version of the original summary (Fig.1). Compared to the original interpretation (Fig. 1) the term granulite has been omitted and a more precise sub-division into tonalite/tonalitic gneisses and granite/granitic gneisses has been introduced.

When comparing thin-sections of cuttings with those from surface samples it is difficult to see any clear similarities concerning composition and texture. However, considering the reinterpreted logs in Fig. 5, the most conspicuous log break is at approximately 550 m. This may correlate with the contact between the upper and middle part of the Jæren Nappe Complex as seen in Fig. 2. The upper part of the nappe complex comprises gneisses, amphibolite, marble and calc-silicate gneiss. This may be equivalent to the mica gneiss and minor calcite marbles of the NSD-1 well. The internal thrust fault of the nappe complex, separating the middle and lower parts, is more difficult to detect in the log interpretations. The fault zone is most probably located in the interval 900 to 950 m. Below this, the dominating rocks are more granitic compared with those above, which are dominated by more tonalitic and amphibolitic rocks. Prominent log breaks are found at 900 and 950 m. These are accompanied by fracturing as seen from the formation micro scanner log. At 950 m there is also a shift from tonalitic gneiss to underlying porphyritic granite.

Surface exposures are rare in the area, and it is difficult to correlate the geology penetrated by the NSD-1 with the previously mapped surface geology.

The well does not penetrate the contact between the Jæren Nappe Complex and the basement.

Acknowledgements

Norsk Agip for financial support for fieldwork and thin-section preparation. Knut Kirkemo, Øystein Nordgulen and Alvar Braathen for critical comments on the manuscript.

7. REFERENCES:

Birkeland, T. 1975: Western Karmøy, an integral part of the Precambrian basement of south Norway. *Norges Geologiske Tidsskrift, 55,* 213-241.

Birkeland, T. 1981: The geology of Jæren and adjacent districts. A contribution to the Caledonian nappe tectonics of Rogaland, southwest Norway. *Norsk Geologisk Tidsskrift,* 61, 213-235.

Dresser Atlas 1983: *Log interpretation charts.* Dresser Atlas Publication.

Gearhart, Inc. 1983: *Formation Evaluation Data Handbook.* Gearhart Inc. Publication.

Jorde, K., Sigmond, E.M.O. & Thorsnes, T. 1995: STAVANGER. Berggrunnsgeologisk kart 1:250 000. *Norges geologiske undersøkelse.*

Rider, M.H. 1986: *The geological interpretation of well logs.* Blackie and Son Limited, Bishopbriggs, Glasgow. 175pp.

Schlumberger 1985: *Log Interpretation Charts.* Schlumberger Publication.

Serra, O. 1972: *Diagraphies et stratigraphie.* Mem. BRGM, Fr., No. 77, 775-832.

Serra, O. 1979: *Diagraphies différées. Bases de l' interprétation. Tome 1: Acquesition des données diagraphiques. Bull. Centre Rech. Expl.-Prod. Elf Aquitaine, Mem.* 1, Technip, Paris, 328.

APPENDIX 1

TH95-01
MESO:
White-pink, medium grained, foliated. Feldspar porphyroclasts (<1cm), reddish weathering, small amounts of mafic minerals.
Light coloured.
MICRO:
35% quartz, ribbon texture, defining foliation.
35% K-feldspar
25% plagioclase, albite porphyroblasts, rounded anhedral crystals, parallel growth, combined Carlsbad-twinning, some with myrmekite texture.
Albite porphyroblasts.
Smaller zones with grain reduction/crushing.
Generally very little mica.
Accessory minerals:
Biotite
1% epidote, large primary grains
1% muscovite, lamellar aggregate around the pophyroclasts.
CONCLUSION: Protomylonitic porphyry granite.

TH95-02
MESO:
Dark grey with light coloured spots, fine grained, some larger feldspar crystals (2-3 mm).
MICRO:
70% hornblende, extinction 12-17dg, generally anhedral, but some euhedral crystals.
25% plagioclase
1-2% biotite, as needles of both euhedral an anhedral crystals, late growth.
Accessory minerals:
Epidote
Sphene/leucoxene, generally anhedral, some oxidation.
Weak parallel growth of minerals.
CONCLUSION: Amphibolite

TH95-03
MESO:
Grey quartzitic, fine to medium grained, weak foliation defined by scattered mafic minerals.
MICRO:
40% quartz
20-25% plagioclase, zoned grains.
15-20% low microcline
1-2% hornblende pleochroitic in strong green to yellow colours.
Accessory minerals:
Epidote, euhedral crystals with allanite nucleus, non pleocroitic, yellow interference colour, extinction

parallel to cleavage,
Sphene, euhedral crystals, brownish, non pleochroitic or masked, extinction 3-4dg, small inclusions of rounded quartz grains.
Heterogranular, weak mineral elongation.
CONCLUSION: Leuco granodiorite (?)

TH95-04
MESO:
Greenish rock, medium grained, yellow to green andradite, quartz veins.
MICRO:
75% epidote, the main mineral, interlocking, subhedral to anhedral crystals, twinning.
10% quartz, recrystallised void filling mineral.
10% microcline
Accessory minerals:
1-2% calcite, single crystals.
1% amphibole, altered, green to colourless.
<1% plagioclase
<1% biotite
<1% apatite
CONCLUSION: Calc epidozite. No real rock, but a result of segregation.

TH95-05
MESO:
Light white-grey, fine grained, weakly foliated, scattered mafic grains, feldspathic laminas more yellow coloured.
MICRO:
50% quartz
30% plagioclase as porphyroclasts.
10% microcline and alkali feldspar with saussuritisation.
5% clinozoisite in columnar aggregates.
2% biotite
Accessory minerals:
Muscovite, colourless, straight extinction
Sphene, diamond shaped?
CONCLUSION: Aplitic vein of granodioritic composition.

TH95-06
MESO:
Greyish, fine to medium grained, well foliated, 1mm thick quartz and feldspar rich laminas, some biotite, the rock is occurring close to lime silicate gneisses, may be of a sedimentary origin.
MICRO:
60-65% quartz, ribbon texture.
15-20% clinzoisite, blue interference colour, oblique extinction.
10% biotite, brown.
1% microcline
Accessory minerals:

Plagioclase
Calcite
Apatite, colourless.
Sphene, larger rounded grains, clasts.
Opaques
Biotite flakes defining weak S-C structures around larger grains of clinozoisite.
CONCLUSION: Feldspathic quartz mica gneiss.

TH95-07
MESO:
Black to dark green, medium grained, some pyrite, some biotite and other mafic minerals as matrix, feldspar grains 3-4mm, weathering around feldspar grains.
MICRO:
50% amphibole
30-40% plagioclase; anorthite, anhedral to rounded porphyroblasts with inclusions of biotite, amphibole and plagioclase, elongated needles of biotite in plagioclase parallel with twinning.
2-4% biotite, brown to yellow, tabular subhedrale to euhedral crystals.
2-3% opaques
Accessory minerals:
Apatite, colourless, grey coloured birefringence.
Sphene, colourless, rhombic, strong light green/yellow interference colour, straight to weakly oblique extinction.
Ilmenite?
Pyrite? opaque, cubic to rhombic, blastic.
CONCLUSION: Amphibolite

TH95-08
MESO:
Light greyish, medium grained, foliated, rich in quartz and feldspar with foliation defined by mafic minerals.
MICRO:
45% quartz, anhedral to subhedral crysts, both as interlocking matrix and with elongated ribbon texture.
30% low microcline.
10% epidote
10% hornblende, green pleochroitic.
1-2% plagioclase (oligoclase), saussuritisation.
Accessory minerals:
Calcite
Apatite
Biotite
Opaques
CONCLUSION: Alkali feldspar granite

TH95-09
MESO:
Grey to weakly pink, fine to medium grained, foliated, alternating darker and lighter band, rusty weathering along mica layers, small red garnets.
MICRO:

70-80% quartz, ribbon texture.
15-20% epidote, colourless, non pleochroitic, oblique to straight extinction, interference colours yellow-purple-blue, moderate relief.
<5% garnets, inclusions of euhedral quartz, older texture preserved.
3-5% hornblende, dark green
Accessory minerals:
<1% opaques
Poikiloblastic, nematoblastic matrix.
Moderately foliated.
CONCLUSION: Meta-arkose

TH95-010
MESO:
Black, medium-grained, red garnets 1-2 mm, quartz veins, no marked foliation.
MICRO:
85-90% hornblende, green pleochroitic, interlocking subhedral and anhedral crysts.
5-10% garnets, brown coloured, as poikiloblasts with inclusions of quartz and hornblende, sometimes having a cloudy appearance.
1-2% quartz, recrystallised.
Accessory minerals:
1% opaques
Plagioclase, saussuritisation along twinnings.
Discrete zones of cataclasis with aligned micro-fractures.
CONCLUSION: Garnet amphibolite

TH95-011
MESO:
Yellow-white, medium-grained, sugary, loosely cemented, mainly calcite.
MICRO:
Granoblastic-elongate texture, elongated grains define a weak foliation, saccaroidal texture with some subhedral to euhedral calcite crystals.
>95% calcite
Plagioclase, with intergrowth of calcite
Alkalifeldspar, with inclusions of epidote.
(Quartz, elongated anhedral grains, but also euhedral.)
Accessory minerals:
Clinozoisite, subhedral grains, often at grain contacts, but also as inclusions in calcite.
Apatite, rounded colourless grains, grey birefringence.
CONCLUSION: Limestone marble

TH95-012
MESO:
Greyish white to weakly bluish with darker grains, medium grained, weakly foliated, scattered larger amphibole grains, some biotite.
MICRO:
35-40% quartz, recrystallised.

5% microcline
12-15% amphibole, green, tightly spaced cleavage, porphyroblasts, some alteration.
25-30% plagioclase, albite as porphyroblasts.
5-8% calcite, anhedrale, cuspate grain contacts, void filling mineral.
Accessory minerals: 4-5%
Biotite
Apatite
Garnet, colourless, but isotropic under crossed polars.
Sphene
Opaques
Weak foliation defined by alignment of biotite crystals.
CONCLUSION: Granodiorite-tonalite

TH95-013
MESO:
Fine grained greenish matrix with coarse grained porphyroclasts, clast in limestone marble, epidote?
MICRO:
55% epidote
40% plagioclase, large crystals.
Accessory minerals: 5%
Zoisite/clinozoisite
CONCLUSION: Saussuritised gabbro, may be a meta-gabbro or a meta-volcanite, large plagioclase crystals may indicate a coarse grained protolith.

TH95-014
MESO:
Medium grained, grey, rich in mica and foliated, some quartz, biotite and white mica.
MICRO:
55-60% quartz, fine grained, xenoblastic.
8-10% biotite
5-6% muscovite, colourless, straight extinction, late growth.
5% plagioclase
Accessory minerals:
Apatite
Microcline
Opaques
CONCLUSION: Muscovite biotite gneiss

TH95-015
MESO:
White-pink, fine to medium grained, massive and unfoliated, small red garnets 1-2 mm.
MICRO:
50% quartz
40% plagioclase, as porphyroblasts, some crystals are zoned.
5% microcline, as porphyroblasts.
2-3% muscovite

Accessory minerals: <1%
Garnets
Patch perthite
Opaques
Apatite
Weak sericitisation in some of the feldspar porphyroblasts.
CONCLUSION: Leucogranitic dyke

TH95-016
MESO:
Grey/green to black, fine grained, foliated, needle-like green hornblende, biotite.
MICRO:
80-85% hornblende, elongated anhedral, some subhedral, dark green to yellow pleochroitic, inclusions of rounded quartz grains.
10-15% quartz, sutured grains as matrix.
2-3% opaques
Accessory minerals:
Biotite
Sphene
CONCLUSION: Amphibolite schist

TH95-017
MESO:
Greyish, medium grained, foliated, red garnets (<5 mm) and hornblende (3-4 mm) in a matrix rich in quartz and feldspar.
MICRO:
50-55% quartz
15-20% amphibole, green, porphyroclasts with inclusions of quartz.
3-4% low microcline.
2-3% plagioclase (oligoclase)
5-6% garnets, porphyroclasts.
15% biotite
Accessory minerals: 2-3%
Sphene
Apatite
Matrix of fine grained quartz, biotite and some amphibole.
CONCLUSION: Garnet-hornblende amphibolite

TH95-018
MESO:
White to yellow/white, medium grained, foliated, quartz-feldspar rich lamina 1-2 mm and thinner green mica rich lamina, stretching lineation.
MICRO:
25-30% quartz, recrystallised with ribbon texture in matrix.
10% plagioclase, porphyroclasts.
35% microcline, porphyroclasts.

5-10% K-feldspar, saussuritisized, porphyroclasts, highly strained with deformation lamellae.
5% biotite
8-10% muscovite
Accessory minerals: <1%
Calcite
Apatite
Lenses defined by biotite and muscovite surround the porphyroclasts.
Very fine grained matrix rich in feldspar, quartz, biotite and muscovite.
Generally very saussuritised feldspar.
CONCLUSION: Granodiorite

TH95-019
MESO:
Brownish mica rich, medium grained, foliated porphyroclastic, rich in biotite, bluish phenocrystals (2-3 mm).
MICRO:
60% calcite, saccaroidal to sutured.
30% quartz, ribbon texture, recrystallised.
5-10% plagioclase, poikiloblastic, with inclusions of quartz, biotite, and opaques.
Accessory minerals:
0,5% biotite
<0,5% opaques, weakly red coloured along the margins.
Muscovite
Clinozoisite, strong blue interference colours
moderate foliation defined by biotite, deflected around plagioclase porphyroclasts, zones with sutured fine grained quartz.
CONCLUSION: Calc silicate gneiss

TH95-020
MESO:
Grey massive, fine grained matrix with needles and more rounded grains of feldspar (red weathering colour)(<5 mm), fresh looking.
MICRO:
75-80% plagioclase (labradorite/bytownite), subhedral prismatic and tabular crystals, saussuritisized with zoisite/clinozoisite.
20-25% opaques
Alignment of tabular and prismatic crystals of plagioclase in a very fine grained matrix. The plagioclase is very saussuritised, and some porphyroclasts are completely overgrown by zoisite/clinozoisite.
The dyke is cut by fractures with calcite.
CONCLUSION: Porphyritic diabase

TH95-021
MESO:
Yellow/grey, medium grained, sugary, quartz and feldspar, biotite.
MICRO:
30% quartz
50% plagioclase, some grains with saussuritisation.

8-10% microcline, some grains as phenocrystals.
5-7% biotite
3% zoisite/clinozoisite
Accessory minerals: 1%
Apatite
Opaques
Granular with generally lobate grain contacts.
CONCLUSION: Granodiorite

TH95-022
MESO:
Grey with white spots, fine grained, foliated, white mica, biotite.
MICRO:
40% quartz
25% plagioclase
10% K-feldspar, zoned crystals, often with deformation lamellae.
10-15% biotite, subhedrale crystals, nematoblastic.
10% muscovite, growing over biotite, subhedral tabular crystals, nematoblastic.
Accessory minerals:
Apatite, both anhedral and subhedral crystals.
CONCLUSION: Granodiorite

TH95-023
MESO:
Greyish green phyllite, folded and crenulated, thin alternating light and dark coloured laminae, some rusty weathering, quartz veins.
MICRO:
Quartz
Muscovite
Accessory minerals:
Opaques, defining the foliation in the quartz rich laminae.
Crenulation of alternating quartz rich and mica rich layers.
CONCLUSION: Phyllite

TH95-024
MESO:
Grey to white spotted, medium grained, weakly foliated, rich in quartz and feldspar, white mica.
MICRO:
30% quartz, recrystallised, interlocking grains.
40% plagioclase porphyroclasts, with strong saussuritisation, numerous inclusions of quartz and mica.
15% muscovite
10% biotite
Accessory minerals:
Calcite
Opaques, probably arsenopyrite.
Epidote, probably with allanite nucleus.

Zoisite/clinozoisite
Apatite
Weak augen texture with foliation of mica curving around porphyroclasts of plagioclase.
CONCLUSION: Porphyric metatonalite

TH95-025
MESO:
Grey weakly pink, medium to coarse grained, foliated with scattered biotite flakes, rich in quartz and feldspar, gneissic.
MICRO:
40% quartz, weak ribbon texture in matrix, mosaic.
35% plagioclase, rounded phenocrystals, saussuritised.
20% low microcline.
Accessory minerals:
<1% opaque
Biotite, pleochroitic yellow-green to brown , tabular to prismatic, in pressure shadows of plagioclase.
Muscovite, colourless, bladed.
CONCLUSION: Monzogranitic gneiss

TH95-026
MESO:
Grey to white, medium to coarse grained, as nr 25 but less foliated and less pink coloured feldspar, granite
MICRO:
Microcline, overprinted with strong saussuritisation.
55% plagioclase, overprinted with strong saussuritisation.
25% quartz, clusters of recrystallised grains.
3-4% biotite, pleocroitic in brown.
Muscovite? extinction nearly straight on cleavage.
Accessory minerals:
Zoisite/clinozoisite
Apatite, rounded grains.
Opaques
CONCLUSION: Tonalitic gneiss

APPENDIX 2

Cuttings under binocular
Meter:

563 m
Very fine grained, dark grey rock.
Large amounts of mica and mafic minerals in a quartz rich matrix.
Needles of amphibole in quartz.
Areas with clusters of greenish minerals similar to quartz.
Biotite.

639 m
Dark grey rock with more light coloured grains of feldspar.
Clear quartz.
Feldspar.
Amphibole.
Fine grained chlorite in aggregates.
Biotite
Muscovite

675 m
Light grey rock: light coloured feldspar with mafic minerals in a greyish matrix.
Blue-grey quartz.
Pink feldspar.
Grains of calcite with chlorite coatings on fracture surfaces.
Amphibole
Biotite
Muscovite

686 m
Dark grey rock with scattered light coloured minerals.
Quartz rich with very little feldspar.
Some grains of calcite with chlorite.
Amphibole
Biotite
Chalcopyrite?

698 m
Feldspathic rock with mafic minerals.
Pink feldspar dominating over quartz.
Yellow/smoke coloured grains of quartz/feldspar?
Some grains of white feldspar with lineations in chlorite coatings.

Amphibole
Biotite

716 m
Light coloured rock with some grains of mafic minerals.
Pink feldspar with some red-coloured grains.
Clear quartz.
Sugary white calcite with chlorite.
Scattered grains of amphibole? in darker quartz rich matrix.
Biotite
Light coloured mica (muscovite).

719 m
Generally light coloured rock.
Clear quartz with flakes of biotite and white mica (muscovite).
Sugary white calcite with lineations on polished surfaces of chlorite.
Some grains with light green coloured aggregates.

722 m
A more coarse-grained, dark and speckled rock.
Pink feldspar.
Some grains of white calcite.
Yellow coloured crystals of calcite (?) together with biotite.
Quartz rich.
Amphibole
Biotite
Muscovite

903 m
Clear bluish to whitish quartz.
Amphibole
Light coloured green chlorite in aggregates.
Brownish biotite.
Rusty spots indicative of oxides.
Pyrite?

1174 m
Quartz rich rock.
White feldspar.
Grains of biotite in quartz, speckled appearance.
Some grains of sugary white calcite.
Opaques, rusty weathering, chalcopyrite?

1183 m
Quartz- and feldspar-rich rock.
Quartz grains with smaller biotite that defines the foliation.
Grain of brownish red quartz-like mineral with inclusions of mafic minerals.
Grains of calcite with lineations in chlorite coatings.
Grains with a light greenish colour, amphibole?
White mica in aggregates.

1192 m
Fine-grained rock rich in mica.
Abundant white mica.
Grains of amphibole.
Some white grains of feldspar.
Fine-grained quartz with mica, also smoky coloured quartz.
Possibly small garnets in quartz which are brownish red and fractured.
Aggregate of fine-grained greenish chlorite, possibly together with white sugary calcite.

1198 m
As at 1192m, but with more calcite present.
Generally fine-grained quartz with mica.
Nearly no amphibole.
Mafic minerals represented by biotite in a matrix of quartz.

1201 m
Calcareous rock, with abundant white sugary calcite grains with smaller inclusions of a darker mineral.
Garnets in quartz.
Fine-grained quartz with small darker biotite grains.
Flakes of white mica.

1213 m
Light coloured rock.
One part consisting of fine-grained quartz with grains of biotite, and one part of limestone which is white and sugary with lots of white mica and darker grains.

1216 m
Quartz grains with biotite and red garnets.
Pale green platy mineral, similar to actinolite in appearance?
Greenish feldsparlike grains.
Rich in white and dark coloured mica.

1228 m

Medium grained and rich in quartz.
Grains of calcite with tiny inclusions of quartz and chlorite coatings.
Scattered flakes of biotite in aggregates of quartz.
Aggregate of red grains that have a rusty weathering colour, garnets?

1237 m
Abundant white mica.
Small grains of quartz with darker mica, biotite and some small garnets.
Some darker grains with amphibole/biotite/quartz.
Some darker grains with a dark green colour.
Very little calcite.

1240 m
Generally high content of white mica.
Large flakes of white mica.
Some grains of white sugary limestone.
Smaller grains of fine-grained quartz with grains of biotite.
Abundant feldspar and a dark green mineral.

Fig. 3 Electrical logs from the Agip NSD-1 well at Tananger and their interpretations in the interval 475-1100 m.

97.176

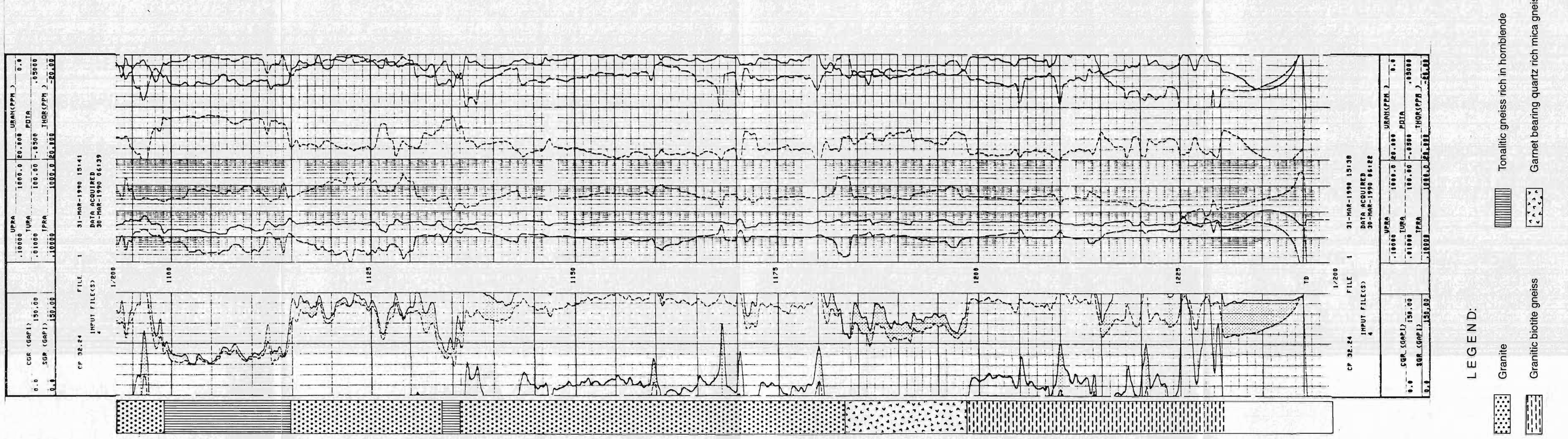

Fig. 4 Electrical logs from the Agip NSD-1 well at Tananger and their interpretations in the interval 1100-1230 m.

97.176